CELL REGULATION, Vol. 2, 861–874, November 1991

Specific association of an M-phase kinase with isolated mitotic spindles and identification of two of its substrates as MAP4 and MAP1B

Robert M. Tombes,* John G. Peloquin, and Gary G. Borisy
Laboratory of Molecular Biology
University of Wisconsin
Madison, Wisconsin 53706

Isolated mammalian (Chinese hamster ovary [CHO]) metaphase spindles were found to be enriched in a histone H1 kinase whose activity was mitotic-cycle dependent. Two substrates for the kinase were identified as MAP1B and MAP4. Partially purified spindle kinase retained activity for the spindle microtubule-associated proteins (MAPs) as well as brain and other tissue culture MAPs; on phosphorylation, spindle MAPs exhibited increased immunoreactivity with MPM-2, a monoclonal antibody specific for a subset of mitotic phosphoproteins. Immunofluorescence using an anti-thiophosphoprotein antibody localized in vitro phosphorylated spindle proteins to microtubule fibers, centrosomes, kinetochores, and midbodies. The fractionated spindle kinase was reactive with anti-human $p34^{cdc2}$ antibodies and with an anti-human cyclin B but not an anti-human cyclin A antibody. We conclude that spindle MAPs undergo mitotic cycle-dependent phosphorylations in vivo and associate with a kinase that remains active on spindle isolation and may be related to $p34^{cdc2}$.

Introduction

The phosphorylation of key structural proteins by mitotic cycle-regulated protein kinases, such as $p34^{cdc2}$, is believed to stimulate the fundamental nuclear changes associated with the G2/M transition (Moreno and Nurse, 1990; Nurse, 1990). Several important mitotic proteins have been identified as substrates of purified $p34^{cdc2}$ (Moreno and Nurse, 1990) and include the lamins (Heald and McKeon, 1990; Peter *et al.*, 1990b; Ward and Kirschner, 1990), histone H1 (Langan *et al.*, 1989), pp60 c-*src* (Shenoy *et al.*, 1989), nucleolin (Belenguer *et al.*, 1990; Peter *et al.*, 1990a), and vimentin (Chou *et al.*, 1990). Genuine physiological roles for some of these $p34^{cdc2}$-specific phosphorylation sites have been recently demonstrated for lamins A and C during the disassembly of the nuclear lamina (Heald and McKeon, 1990; Ward and Kirschner, 1990).

Nonetheless, there are many other undefined mitotic phosphoproteins and cellular functions that undergo abrupt cell-cycle transitions coincident with $p34^{cdc2}$ cycles. For instance, pleiotropic changes in microtubule (MT)[1] and spindle behavior occur as cells enter mitosis. MT nucleating capacity at the centrosome increases fivefold at the onset of mitosis (Kuriyama and Borisy, 1981) and abruptly is lost as chromosomes initiate poleward movement at anaphase onset (Snyder *et al.*, 1982), in synchrony with the activation and inactivation of $p34^{cdc2}$ kinase (Draetta and Beach, 1988). MT dynamics are increased as cells enter mitosis (Belmont *et al.*, 1990). Changes in MT dynamics and architecture, similar to those occurring at the interphase/mitosis transition, have been observed after the introduction of active $p34^{cdc2}$ into cells or extracts (Lamb *et al.*, 1990; Verde *et al.*, 1990). In addition, $p34^{cdc2}$ co-localizes with the mitotic spindle in a variety of cells (Bailly *et al.*, 1989; Riabowol *et al.*, 1989; Rattner *et al.*, 1990) and is thought to be a chromatin-associated kinase (Langan *et al.*, 1989). However, genuine spindle or MT-associated substrates of $p34^{cdc2}$ or other M-phase kinases have yet to be defined.

The isolated mitotic spindle presents an opportunity not only to identify and characterize

* Present address: Department Biological Sciences, Clemson University, Clemson, SC 29634.

[1] Abbreviations used: ATP-γ-S, adenosine 5′-O-(3-thiotriphosphate); BSA, bovine serum albumin; cAMP, cyclic AMP; CHO, Chinese hamster ovary; DAPI, 4′,6-diamidino-2-phenylindole; DTT, dithiothreitol; EGTA, ethylene glycol-bis(β-aminoethyl ether)-*N,N,N′,N′*-tetraacetic acid; HEPES, *N*-2-hydroxyethylpiperazine-*N*′-2-ethanesulfonic acid; MAP, microtubule-associated protein; MT, microtubule; NEM, N-ethyl maleimide; PKA, protein kinase A; SDS, sodium dodecyl sulfate; TBS, Tris-buffered saline; Tris, tris(hydroxymethyl)aminomethane.

© 1991 by The American Society for Cell Biology

mitotic kinases and their substrates in a purified mitotic organelle, but to assign location and define function to such phosphoproteins in a system amenable to functional assays. The general importance of such phosphorylations has already been implied because specific spindle proteins, including MAP4, MAP1B, and other unidentified antigens, show phosphorylation and dephosphorylation cycles parallel with M-phase, as detected by a monoclonal antibody reactive with mitotic phosphoprotein epitopes. This antibody, known as MPM-2, has localized phosphoproteins at centrosomes, kinetochores, and along spindle fibers in fixed cells (Vandre *et al.,* 1984), and isolated Chinese hamster ovary (CHO) mitotic spindles (Vandre *et al.,* 1991); is a ubiquitous eukaryotic M-phase epitope (Vandre *et al.,* 1986; Keryer *et al.,* 1987; Engle *et al.,* 1988; Wordeman *et al.,* 1989); and can block both mitosis (Davis *et al.,* 1989; Kuang *et al.,* 1989) and the nucleation of MTs from the centrosome in vitro (Centonze and Borisy, 1990). The kinase(s) responsible for conferring this epitope has not been identified, but spindle- or centrosome-associated kinases have been reported (Zieve and Solomon, 1982; Nigg *et al.,* 1985; Dinsmore and Sloboda, 1988; Kuriyama, 1989), although they have not been extensively characterized.

We have found that isolated, purified spindles are enriched in a histone H1 kinase that specifically associates with its substrates, including MAP4 and MAP1B; the phosphorylation of those proteins by adding back the fractionated spindle kinase results in augmented MPM-2 immunoreactivity. By immunolocalization, the spindle kinase substrates were localized to the kinetochore fibers, spindle poles, and kinetochores. Our results suggest that the spindle kinase, which is cross-reactive with antibodies to $p34^{cdc2}$, operates in close association with its spindle substrates at discrete sites, perhaps as a means to closely coordinate their function during the mitotic cycle.

Results

Identification of spindle-associated kinase and substrates

Purified mitotic spindles, as expected, contained primarily α and β tubulin, plus additional polypeptides (Figure 1, lane 1). The MPM-2 antibody detected a limited group of mitotic phosphoproteins in spindles (lane 2), as previously shown (Vandre *et al.,* 1984, 1991). The apparent pattern of MPM-2 immunoreactive spindle bands differs in this report from the reports referenced above, primarily due to the use of 4–12% gradient polyacrylamide gels in place of 7.5% nongradient gels. When spindles were incubated with MgATP-γ-^{32}P, an endogenous kinase activity phosphorylated almost all of the MPM-2 reactive proteins, as well as some others (lane 3). This kinase activity showed saturable kinetics with respect to time, substrate, and ATP concentration, and the spectrum or degree of ^{32}P incorporation was not altered by 10 μM cyclic AMP (cAMP), 10 μM cyclic GMP, or 20 μM free Ca^{2+} with or without 5–15 μg/ml bovine brain calmodulin (data not shown). Nonetheless, kinase assays were typically run in the presence of the peptide inhibitor of the cAMP-dependent protein kinase and ethylene glycol-bis(β-aminoethyl ether)-*N,N,N',N'*-tetraacetic acid (EGTA) as well as phosphatase inhibitors (see Materials and methods). The kinase activity persisted in spindles through three successive centrifugal washes (lanes 6–8). Further evidence for a specific association of the kinase activity with the spindle was demonstrated by the five- to sixfold increase in its specific activity when spindles were purified from cell lysates (Table 1).

Two of the major endogenous spindle kinase substrates were identified as MAP4 and MAP1B

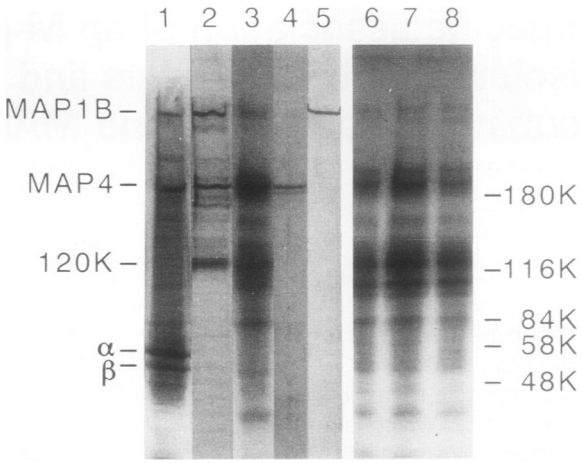

Figure 1. **Detection of spindle kinase and identification of substrates.** One microgram (unless otherwise indicated) of CHO spindles were phosphorylated with 1 μM MgATP-γ-^{32}P for 30 min (see Materials and methods) and electrophoretically separated on a 4–12% polyacrylamide SDS gel. Lane 1, silver stain; Lane 2, MPM-2 immunoblot (10 μg); Lane 3, autoradiogram of ^{32}P-labeled spindles in lane 2; Lane 4, MAP4 immunoblot (10 μg); Lane 5, MAP1B (MAP5) immunoblot (10 μg); Lanes 6–8, autoradiograms of spindles, phosphorylated after each of three successive washes. α and β refer to tubulin subunits. 120K is the major ^{32}P and MPM-2 labeled, but unidentified, band. Standards are as indicated in M_r (K = 10^3).

Table 1. Fractionation of spindle histone H1 kinase

Fraction	fmoles/min	μg	pmoles/min/mg
Mitotic lysate	575 000	8500	67
Mitotic supernatant	484 000	8000	60
Spindles	26 500	80	330
Spindle extract	25 000	20	1250
DEAE peak	10 250	4	2600
S300 peak	4 100	1	4100

This purification was normalized for 10^8 synchronized metaphase CHO cells (see Materials and methods). Mitotic lysate is the cell lysate before removal of spindles by centrifugation at 2000 × *g* and mitotic supernatant is after centrifugal spindle removal. Spindle extract is the 0.5 M NaCl extract and column peaks represent the activity in pooled fractions (see Materials and methods). The most purified kinase fraction contained a major protein 65 000 M_r (see Figure 6). Histone H1 kinase activity was by phosphocellulose paper assay.

using a polyclonal antibody directed against CHO MAP4 and a monoclonal antibody against bovine brain MAP1B (Figure 1, lanes 4 and 5). MAP4 is the major MT-associated protein (MAP) in nonneuronal cells and is associated with kinetochore and nonkinetochore fibers in mitotic spindles (Bulinski and Borisy, 1980). MAP4 has been previously identified as one of the major mitotic cycling phosphoproteins (MPM-2 reactive) in isolated spindles (Vandre *et al.*, 1991), and our evidence suggests that the MAP4 immunoreactive band(s) is that which is phosphorylated by the endogenous kinase. We have identified MAP1B as a kinase substrate by the same approach. MAP1B has been found in cultured cells, is believed to be present at centrosomes, and is known to be a phosphoprotein (Vallee *et al.*, 1986). MAP1A may also exist at the centrosome and perhaps throughout the spindle (Bonifacino *et al.*, 1985; DeMey *et al.*, 1987), although our data is inconclusive on the existence of MAP1A in the spindle. Other phosphoproteins, with M_r ($\times 10^{-3}$) of 220, 160, 130, 120, 105, and 80, remain unidentified (Figure 1, lane 3). Of these, the 120 000 M_r spindle phosphoprotein comigrates with the upper band of the CHO1 doublet using a monoclonal antibody against CHO1 (Sellitto and Kuriyama, 1988); however, none of these proteins have been more definitively identified.

The phosphoaminoacids of MAP1B, MAP4, and the 120 000 and the 105 000 M_r phosphoproteins were determined by analysis of ^{32}P-labeled bands excised from one-dimensional sodium dodecyl sulfate (SDS) gels (Figure 2A). Each of these proteins was phosphorylated by the endogenous spindle kinase 95–100% on serine, with the remainder on threonine and no phosphotyrosine (Figure 2B).

Exogenous substrates of the spindle kinase

Exogenous substrates for the spindle kinase were examined for two reasons. First, we wanted to define whether purified brain and interphase tissue culture MAPs could serve as substrates in addition to spindle MAPs. Second, we wanted to find readily available substrates that competed well with spindle substrates to effectively fractionate the relevant spindle kinase. All of the MAP fractions tested, including porcine brain MAPs, cultured cell (HeLa) MAPs, and porcine brain tubulin (Figure 3, A–C, lanes 1–3), contained endogenous kinase activity that could be inactivated by either heat or alkylation (see Materials and methods).

Comparing these additional substrates with the endogenous substrate pattern of spindles alone (lane 8), the high-molecular-weight (HMW) brain MAPs (lane 1) were excellent substrates. This group migrates much more slowly than the 180K M_r standard and includes MAPs 1A, 1B, 2A, and 2B when resolved from each other by separation on low (4%) percentage polyacrylamide gels (see Materials and methods). HeLa MAPs contained some residual β-tubulin (migrating at 55K), which in addition to a 105K MAP were prominent substrates (lane 2). Brain β-tubulin (lane 3) was also a substrate for the kinase

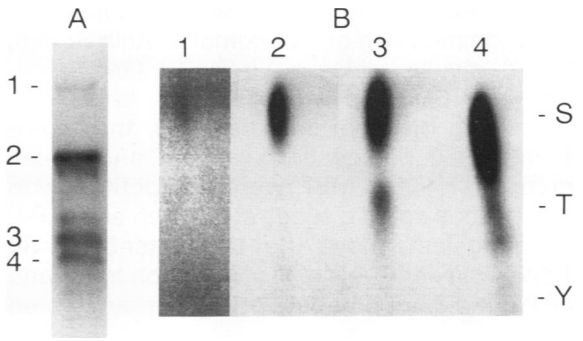

Figure 2. **Phosphoamino acid analysis of spindle phosphoproteins.** (A) Autoradiogram of spindles phosphorylated as in Figure 1, lane 3. (B) Indicated bands (1–4) in (A) were excised from the first dimension, hydrolyzed with 6 N HCl, and electrophoresed on cellulose plates in 5% acetic acid/0.5% pyridine. S, T, and Y indicate positions of ninhydrin-stained phosphoserine, phosphothreonine, and phosphotyrosine standards. Phosphoaminoacid regions were scraped and counted directly or densitometry was used to estimate the following relative contributions of phosphoserine (S) and phosphothreonine (T). Lane 1, MAP1B (100% S); Lane 2, MAP4 (100% S); Lane 3, 120K band (95% S, 5% T); Lane 4, 105K band (95% S, 5% T).

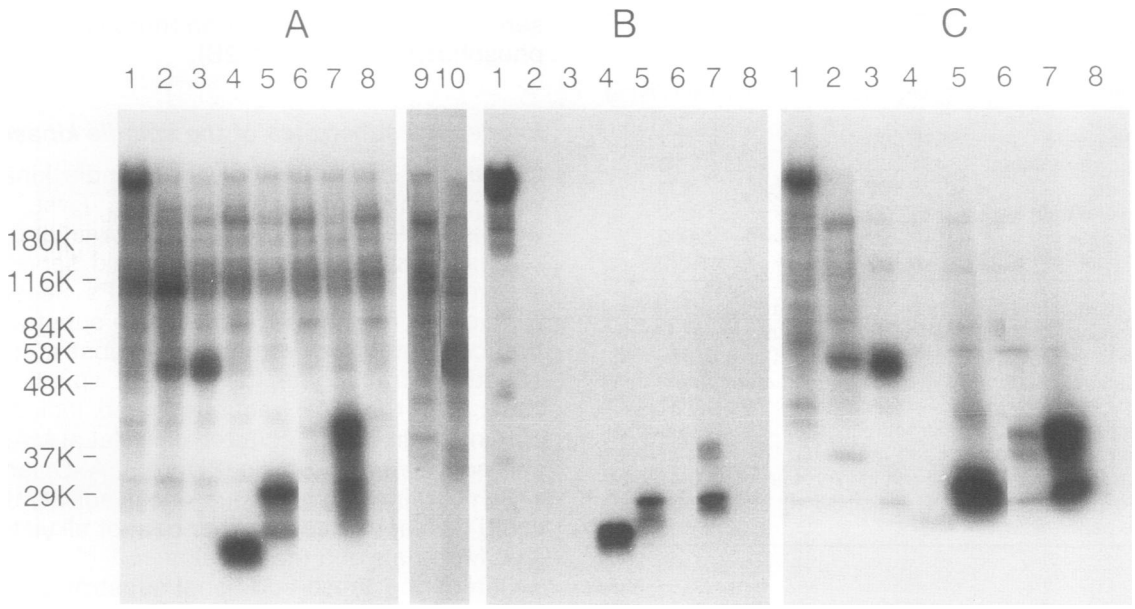

Figure 3. **Spindle protein kinase substrates.** Autoradiograms of various substrates (2 μg) phosphorylated with 1 μM MgATP-γ-^{32}P and either 1 μg isolated spindles (A); comparable amounts of activity of the catalytic subunit of the cAMP-dependent protein kinase (B); or the purified spindle kinase (C) (see Table 1). Within each panel, lanes are from the same exposure so that relative incorporation between substrates can be accurately estimated. Between panels, relative exposures were 2, 1, and 1. Lane 1, porcine brain MAPs; major protein by mass is MAP2; Lane 2, HeLa MAPs; Lane 3, porcine brain tubulin; Lane 4, S6 peptide; Lane 5, myelin basic protein; Lane 6, casein; Lane 7, histone H1; Lane 8, no substrates. Lanes A9 and A10 are from a different experiment showing the accessibility of endogenous tubulin as a substrate after partial salt extraction. The tubulin doublet migrates between standards of 48 and 58K (see Figure 1). Lane A9, spindles, phosphorylated after incubation on ice for 30 min. Lane A10, same spindles, phosphorylated after 30 min on ice with 0.25 M NaCl followed by dilution to final concentration of 0.05 M NaCl. Standards are as indicated in M_r (K = $\times 10^3$).

activity bound to spindles and showed competition with endogenous spindle substrates (compare with lane 8).

Other exogenous substrates tested included a peptide modeled on ribosomal protein S6 (S6, lane 4), myelin basic protein (MBP, lane 5), casein (lane 6), and histone H1 (H1, lane 7). In decreasing order of incorporation, they were H1, MBP, S6, and casein. Like MAP and tubulin fractions, H1 and MBP were competitive with endogenous spindle substrates, such as MAP4, migrating just above the 180K standard. S6 showed similar levels of incorporation to H1 and MBP but did not compete at all. This suggested that
the S6 kinase was not the kinase that phosphorylated endogenous spindle substrates; in agreement, unlike histone H1 kinase, S6 kinase activity was variably present in spindle preparations and the fractionated histone H1 spindle kinase lacked S6 kinase activity (See below).

Despite the propensity of the spindle kinase to phosphorylate exogenous brain or HeLa tubulin, it did not phosphorylate endogenous spindle tubulin (Figure 3A, lane 9) unless spindles were first treated with salt (Figure 3A, lane 10). We interpret this result as indicative of an association of the spindle kinase with its nontubulin spindle substrates, a conclusion further substantiated in later experiments.

We compared the spindle kinase substrate specificity with a known brain MAP kinase, the catalytic subunit of cAMP-dependent protein kinase (protein kinase A or PKA), and found it to be markedly different (Figure 3B). MAP2 was an excellent substrate (lane 1), as expected (Theurkauf and Vallee, 1982), but neither HeLa MAPs (lane 2) nor tubulin (lane 3) were phosphorylated. S6 and MBP were good substrates (lanes 4 and 5), casein was weakly phosphorylated (lane 6), and a lower M_r histone species than that phosphorylated by spindles was phosphorylated by PKA (lane 7). This may represent the different histone H1 isoform known to be favored by PKA (Ajiro *et al.*, 1990). Autophosphorylation of PKA was undetectable (lane 8) at this exposure or at 100-fold longer exposures.

The major histone H1 kinase purified from spindles (see ***Fractionation of the spindle kinase*** below and Materials and methods) showed a substrate profile closely like that of the spindle

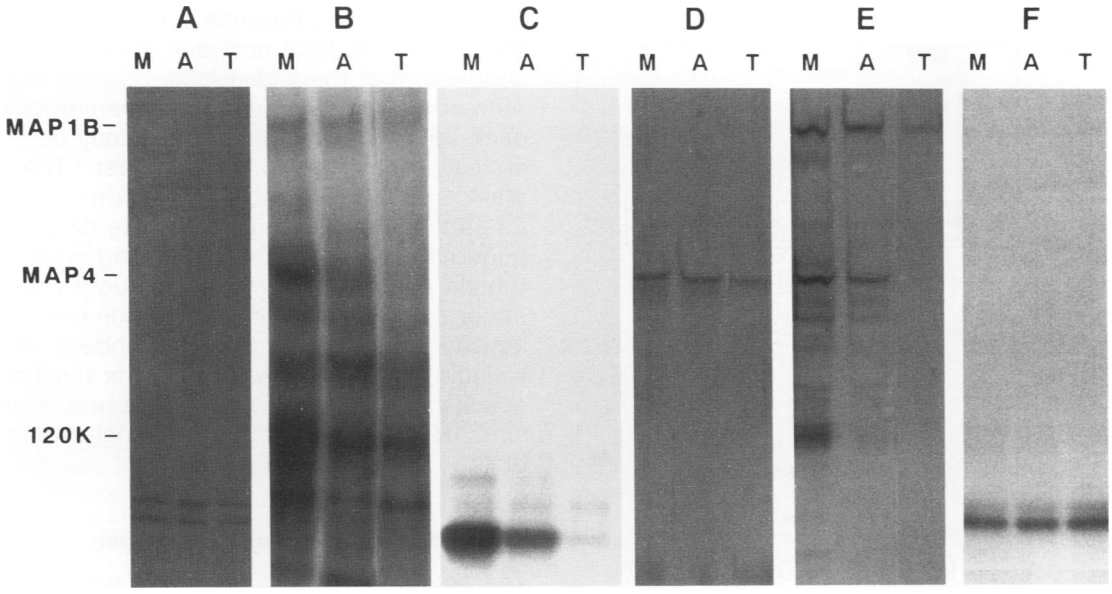

Figure 4. **Mitotic cycle dependency of the spindle kinase.** Spindles were phosphorylated with or without exogenous substrates for 30 min as in Figure 1, except at various times during mitosis (T is time after nocodazole release), including metaphase (M, 10 min), anaphase (A, 20 min), and telophase (T, 40 min). Loadings were 1 μg spindle protein and/or substrate per lane, except for immunoblots that were 10 μg spindle protein. The 4–12% polyacrylamide gradient gel was overrun by 25% to get better separations of high molecular weight bands. Relative exposure times of autoradiograms (B, C, and F) were 50, 1, and 5, respectively. (A) Coomassie stain; (B) autoradiogram of endogenous protein phosphorylation; (C) autoradiogram of exogenous histone H1 phosphorylation; (D) MAP4 immunoblot with anti-CHO MAP4 polyclonal; (E) MPM-2 immunoblot; (F) autoradiogram of exogenous brain tubulin phosphorylation.

kinase and much different from PKA (Figure 3C). Notable differences included diminished incorporation into the 105K HeLa MAP protein (lane 2) and the complete absence of S6 phosphorylation (lane 4). The absence of the endogenous spindle substrates enabled a clearer determination of the degree of phosphorylation into proteins that comigrated with endogenous spindle substrates such as the 105K HeLa MAP, MAP4, and HMW brain MAPs. Autophosphorylation of the spindle kinase was not observed at this exposure (lane 8) or at exposures 100 times longer; at exposures 1000 times longer than shown here, phosphorylated proteins of 55–65K M_r were occasionally observed.

Mitotic cycle dependency of the spindle kinase

Highly synchronous populations of mitotic spindles can be isolated from cells allowed to progress to various stages after release from nocodazole-arrest (Vandre *et al.,* 1991). The synchrony and timing of such populations were verified by analysis of populations of 4′,6-diamidino-2-phenylindole-stained cells fixed at the same time as cells that were lysed for spindles. A 10-min release yields 95% metaphase figures, 20 min yields 65% anaphase, and 30–40 min yields over 95% telophase. The consistency of the mass of the tubulin doublet through such a time course (Figure 4A) revealed that MT-rich spindles could be isolated up to 40 min after release (see anti-tubulin immunofluorescence of the same time course spindles in Figures 10 and 11), although not much later than 40 min. The distribution of spindle morphologies is summarized in Figure 5A.

The phosphorylation of certain spindle proteins, specifically MAP4 and the 120K protein, by the endogenous spindle kinase diminished as soon as anaphase onset, as seen by direct inspection of the autoradiogram (Figure 4B) and more clearly when the ^{32}P incorporation was quantitated (Figure 5B), as described (see Materials and methods). The phosphorylation of exogenous histone H1 also showed a dramatic decrease of >95% by telophase (Figures 4C and 5B) that closely paralleled the decrease in the percentage of cells in metaphase (filled bars in Figure 5A). Even though certain spindle proteins, such as MAP4, decreased by 40–50% in mass as cells progressed toward telophase (Figure 4D), the loss of MAP4 MPM-2 reactivity (Figure 4E) and histone H1 kinase activity dropped by ≥95% starting at anaphase onset

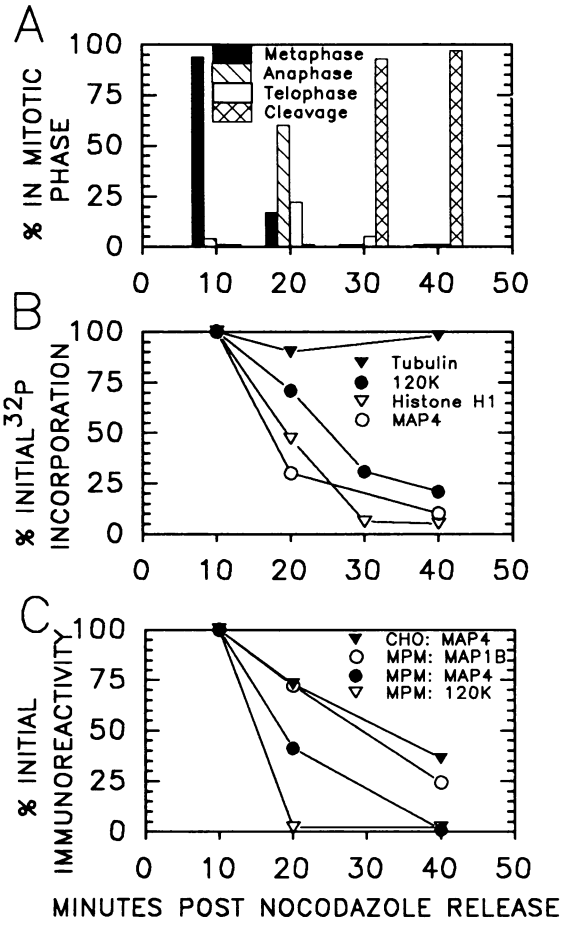

Figure 5. **Quantitation of cell, protein and phosphoprotein mitotic kinetics.** (A) Distribution of cells in mitotic phases at each time point. A portion of synchronized cells at the time indicated after nocodazole release (see Materials and methods) was fixed with 0.05% glutaraldehyde/PBS; simultaneously, the remainder was lysed for the preparation of spindles used in the indicated kinetic experiments. Cells were then stained with DAPI to visualize chromosomes and ≥200 cells counted to assess each mitotic phase. Metaphase cells showed no separation of sister chromatids. Anaphase cells showed both early and late chromatid separation, without cellular constriction. Telophase cells were scored as those showing both early and late signs of cellular constriction. Cleaved cells represented those which had completed constriction. (B) Percent initial ^{32}P incorporation into various proteins relative to metaphase. ^{32}P incorporation was determined by averaging data from the densitometric analysis of autoradiograms (Figure 4) and from excised and directly counted regions of dried gels from several experiments. Initial rate was the incorporation at 10 min (metaphase). (C) Percent initial immunoreactivity of various proteins relative to metaphase. Immunoreactivity was estimated by densitometry, using initial reactivity as that at 10 min. CHO MAP4 represents the quantitated immunoreactivity using the CHO polyclonal antibody against MAP4 (Figure 4D). MPM followed by a protein represents the quantitated immunoreactivity for that protein from the MPM-2 immunoblot in Figure 4E.

(Figure 5C). The difference in the rate of loss of the MPM-2 epitope between spindle proteins suggests that the kinase/phosphatase equilibrium after anaphase onset may vary in vivo for each substrate, i.e., substrates may be differentially accessible to phosphatase. The constant rate of incorporation of ^{32}P into non-MPM-2 reactive proteins throughout the time course (Figure 4B) was also seen with exogenous brain tubulin (Figure 4F). This result suggested that either spindles contain another kinase, whose activity is not mitotic cycle-dependent, or that a single kinase undergoes a change in substrate specificity, losing activity against one group of sites (H1) while retaining it against others (tubulin).

Fractionation of the spindle kinase

To fractionate the spindle kinase, we chose histone H1 as the substrate because it competed well with endogenous substrate phosphorylation and showed the highest level of ^{32}P incorporation. Spindle histone H1 kinase activity was purified by NaCl extraction of spindles, ion exchange, and gel filtration chromatography. The kinase was essentially quantitatively (95%) extracted with 0.5 M NaCl and resolved as a single peak on ion exchange chromatography (Figure 6). Gel filtration yielded a broad peak above 60 000 M_r (data not shown) but still provided a limited degree of purification (Table 1). The distribution of the kinase activity through the purification revealed that most of the cellular histone H1 kinase activity remained soluble; only 5% bound to the spindles. Nonetheless, spindle kinase-specific activity increased at each step of the purification, particularly when spindles were simply centrifuged out of the cellular lysate. Although the DEAE kinase fraction was free of other spindle kinase substrates, the specific activity of the most purified fraction was still about two orders of magnitude less than that of purified mitotic mammalian histone H1 kinase (Brizuela *et al.*, 1989). A silver-stained gel of the DEAE peak pool is shown in the inset in Figure 6 and when compared to whole spindles (lane 1, Figure 1), also reveals the degree of purification. We loaded 20 times the amount of activity used to phosphorylate exogenous proteins (Figure 3) but could still see no more than a few proteins, the most prominent of which was a species migrating at M_r 65K.

Because there is evidence linking the $p34^{cdc2}$ kinase to the mammalian mitotic spindle and centrosomes (Bailly *et al.*, 1989; Riabawol *et al.*, 1989; Alfa *et al.*, 1990; Rattner *et al.*, 1990) and

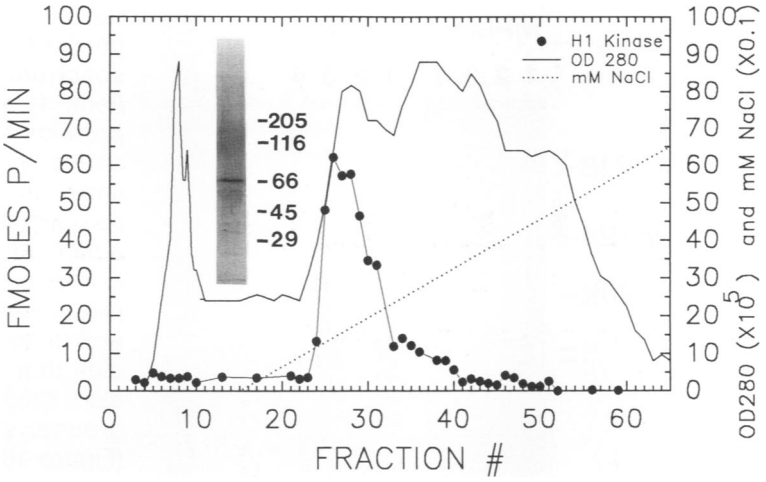

Figure 6. **DEAE factionation of spindle histone H1 kinase.** (A) Spindle extract (See Table 1 and Materials and methods) was chromatographed on DEAE-Sepharose CL-6B at pH 7.4. OD_{280} was by on-line detector and H1 kinase activity (fmoles P/min) was by phosphocellulose paper assay. NaCl (mM) was determined by conductivity measurements. Kinase peak pool was fractions 25–32. Inset reveals the silver staining pattern of a gel of the pooled DEAE peak, with M_r standards indicated ($M_r \times 10^{-3}$).

because, like $p34^{cdc2}$, the spindle kinase lost activity at anaphase onset, we decided to probe spindles and our spindle kinase fraction for $p34^{cdc2}$ and its regulatory subunit, cyclin B (Pines and Hunter, 1990), using polyclonal antibodies against human proteins. Our results, shown in Figure 7, indicate that both $p34^{cdc2}$ and cyclin B species (of appropriate 34 and 56K M_r, respectively) are present in spindles, but that antibodies against cyclin A do not detect any immunoreactive bands (lanes 1–3). The fractionated spindle kinase also contained the same species immunoreactive with anti-$p34^{cdc2}$ and anti-cyclin B (lanes 4 and 5). We observed the same result when different amounts of activity were loaded for each sample or when an alternative antibody directed against the C-terminus of human $p34^{cdc2}$ was used (data not shown). Although the spindle kinase fraction was enriched for a kinase, it was not of sufficient purity to unequivocally conclude that it contained a single kinase species.

Phosphorylation of spindle proteins with purified spindle kinase

To test whether the purified spindle kinase could phosphorylate the same proteins as the endogenous spindle kinase, we added back-fractionated spindle kinase and MgATP-γ-^{32}P to spindles, whose endogenous kinase activity was eliminated by either heating or N-ethyl maleimide (NEM) alkylation (see Materials and methods). We preferred heating because NEM alkylation, although essentially yielding the same results shown here resulted in M_r changes of modified proteins, was less complete and was slower than heating. Our results showed that the substrate reactivity of the spindle kinase was identical to that of the endogenous kinase, except for a band that appeared to comigrate with β-tubulin (Figure 8B, lanes 1 and 3). As with partially salt-extracted spindles (Figure 3), the acquired promiscuity of the solubilized spindle

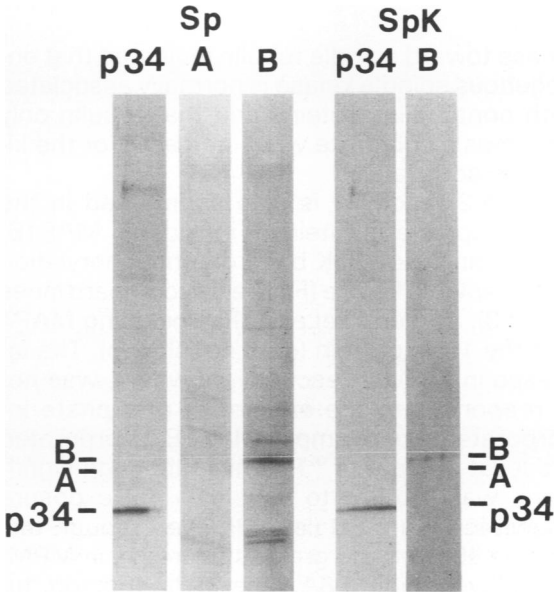

Figure 7. **Identification of $p34^{cdc2}$ and cyclin B but not cyclin A in spindles and in the spindle kinase fraction.** Histone H1 kinase activity (20 000 fmoles/min) from spindles (Sp) and 5000 fmoles/min per lane from the DEAE peak of spindle kinase (SpK) was loaded and run in lanes indicated. Immunoblotting was with a 1:500 dilution of a polyclonal rabbit antibody directed against the entire recombinant human $p34^{cdc2}$ molecule (p34) or a 1:500 dilution of polyclonal rabbit antibodies against recombinant human cyclin A (A) or cyclin B (B). Recombinant standards were run simultaneously but are shown only as indicated migration positions (p34, A and B). Detection was with a biotin/streptavidin-peroxidase system. Another polyclonal antibody directed against the C-terminus of $p34^{cdc2}$ gave similar results.

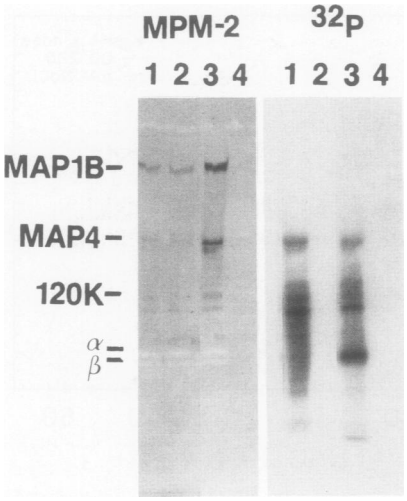

Figure 8. **Phosphorylation of spindle proteins using spindle kinase fraction.** Spindles were phosphorylated with ^{32}P-ATP as in Figure 1 and then processed for: (A) immunoblotting with MPM-2 and (B) autoradiography of the MPM-2 immunoblot in (A) with the following treatments and additions. Lane 1, Spindles alone; Lane 2, heated spindles; Lane 3, heated spindles plus spindle kinase (DEAE peak); Lane 4, spindle kinase alone (DEAE peak).

kinase toward spindle tubulin indicated that endogenous spindle kinase is normally associated with nontubulin proteins and that tubulin only becomes a substrate when at least it or the kinase is soluble.

MPM-2 reactivity is also augmented in the same spindle proteins, including MAP1B, MAP4, and the 120K band on phosphorylation by the spindle kinase (Figure 8A, compare lanes 1 and 3), as were HeLa MAPs, including MAP4 and the 105K protein (data not shown). The increase in MPM-2 reactivity, however, was not in proportion to the amount of phosphate incorporated. For example, MAP1B incorporated the least amount of ^{32}P, which although significant, was too low to appear in the exposure shown in Figure 8B (lane 3), even though this protein showed the greatest increase in MPM-2 reactivity (Figure 8A, lane 3). In addition, tubulin, which is an excellent substrate of the solubilized spindle kinase, did not acquire the MPM-2 epitope (lane 3) nor did histone H1 (data not shown).

Localization of spindle kinase substrates

Adenosine 5′-O-(3-thio-triphosphate) (ATP-γ-S) can be efficiently substituted for ATP as shown by the similar profiles of ^{32}P-phosphoproteins and thiophosphoproteins (Figure 9) detected by immunoblotting with an anti-thiophosphoprotein antibody (Cyert *et al.*, 1988). The thiophosphoproteins (lane 3) showed a more similar spectrum to the ^{32}P-labeled phosphoproteins (lane 1) than to the MPM-2-reactive spindle proteins (lane 4). Some cross-reaction of the antibody with unlabeled spindles is apparent (lane 2) but minor in comparison to labeled spindles and presumably represents cross-reaction with phosphorylated proteins.

Precise localization of these thiophosphoproteins was accomplished by indirect immunofluorescence. As with immunoblotting, spindles that had never been exposed to ATP-γ-S also revealed a weak, but significant background, which was invisible at this exposure (Figure 10D). The signal in thiophosphorylated spindles, however, was strong and precisely localized incorporation, diffusely along the kinetochore fibers and intensely at the poles and kinetochores, the latter colocalizing with the CREST antigens (Figures 10, A–C), which are kinetochore-specific human auto-immune antigens (Bernat *et al.*, 1990). This clearly indicated that these isolated spindles contain at least remnants of the kinetochore, as suspected (Vandre *et al.*, 1991). By immunoblotting spindles, two CREST-reactive spindle antigens ap-

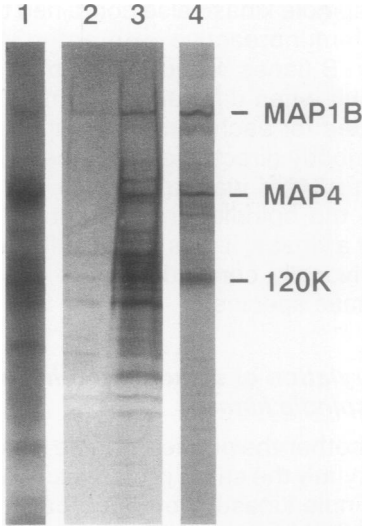

Figure 9. **Detection of spindle kinase substrates with anti-thiophosphoprotein antibodies.** Ten micrograms of spindles per lane were phosphorylated with 50 μM ATP-γ-S, as in Figure 1, and processed for immunoblotting with a monoclonal antibody reactive with thiophosphorylated proteins. For reference, the autoradiogram (lane 1) of an MPM-2 immunoblot (lane 4) of ^{32}P-ATP-labeled spindles is also shown. Lane 1, Autoradiogram of ^{32}P-ATP-labeled spindles; Lanes 2 and 3, anti-thiophosphoprotein immunoblot of (lane 2) unlabeled spindles and (lane 3) spindles labeled with 50 μM ATP-γ-S; Lane 4, MPM-2 immunoblot of spindles.

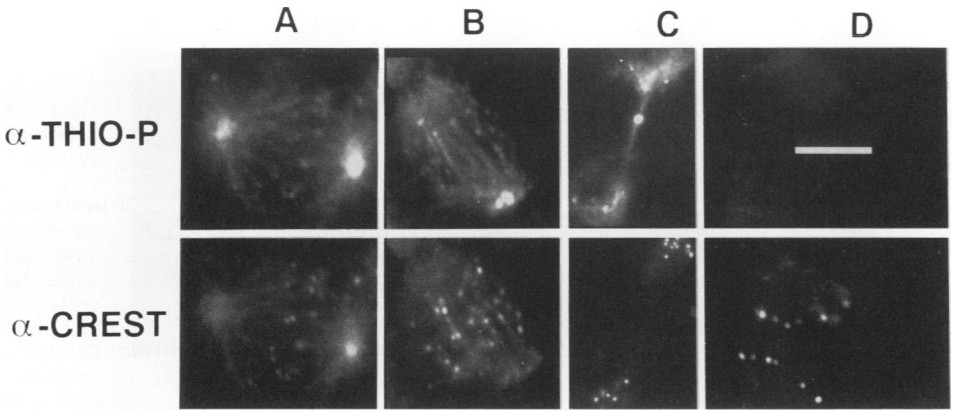

Figure 10. **Immunolocalization of spindle kinase substrates with anti-thiophosphoprotein antibodies.** Spindles were prepared at 10, 20, and 40 min after nocodazole release (See Figure 5), then phosphorylated with 50 μM ATP-γ-S as in Figure 9, centrifuged onto coverslips, fixed with −20°C methanol, and processed for immunofluorescence using in order, the anti-thiophosphoprotein monoclonal antibody (α-THIO-P) and kinetochore-specific human autoimmune sera (α-CREST). Scale bar is 10 μm. (A) Metaphase; (B) Anaphase; (C) Telophase; (D) Metaphase spindle not labeled with ATP-γ-S, but reacted with both THIO-P and CREST antibodies.

pear at around 105 and 75K (data not shown). Telophase spindles showed strong incorporation at the midbody.

As expected from $p34^{cdc2}$ immunoblot reactions of spindles, immunolocalization with anti-$p34^{cdc2}$ and cyclin B antibodies revealed spindle staining. The immunoreactive pattern was similar to MPM-2 and the anti-thiophosphoprotein antibody; it stained poles, fibers, and dots, some of which are probably kinetochores at metaphase and anaphase (Figure 11, A, B, E, and F), and the MT fibers and midbody of telophase spindles (Figures 11, C and G). Staining intensity of both $p34^{cdc2}$ and cyclin B diminished as cells progressed into telophase (Figure 4C and 5B).

Discussion

Our results suggest that a mitotic kinase exists in an active complex with specific protein substrates of the fibroblast mitotic spindle. The phosphorylated metaphase spindle proteins are primarily those previously defined as possessing the mitotically cycling phospho-epitope, MPM-2 (Vandre *et al.,* 1991), and include MAP1B and MAP4. The partially purified spindle kinase can directly confer the MPM-2 epitope to those proteins. The kinase appears to be closely associated with these spindle substrates for the following reasons. First, its specific activity is enriched on spindle purification and it remains bound through multiple washes, indicating the specific association of the kinase with some spindle component. Second, its activity toward these substrates can be competed by exogenous substrates, such as histone H1. Third, the spindle kinase acquires β-tubulin as a substrate only after solubilization, indicating that the kinase has the potential to phosphorylate the major spindle protein, tubulin, but its normal association with spindle MAPs restricts it from doing so. The association of the spindle kinase with its spindle MAP substrates may be comparable with the association of the cAMP-dependent protein kinase with a specific domain of its major MAP substrate, MAP2 (Theurkauf and Vallee, 1982). The spindle kinase identified here can phosphorylate brain MAP2, but the spindle kinase substrates are not phosphorylated by the cAMP-dependent kinase.

The spindle kinase substrates are variably reactive with the MPM-2 antibody. For example, although an excellent spindle kinase substrate, histone H1 does not become MPM-2 reactive on phosphorylation. Some substrates that are heavily phosphorylated show little MPM-2 immunoreactivity (120K), whereas others that are lightly phosphorylated become intensely immunoreactive (MAP1B). We do not interpret this as indicative of multiple kinases, but rather that the MPM-2 epitope is dependent on the amino acid sequences surrounding the phosphorylation site. A similar variance between the incorporation of phosphate into protein and their immunoreactivity with the anti-thiophosphoprotein antibody has been observed (Cyert *et al.,* 1988; our results). These data suggest that (thio)phosphoprotein epitopes would be difficult to define by sequencing single phosphoproteins (Zhao *et al.,* 1989).

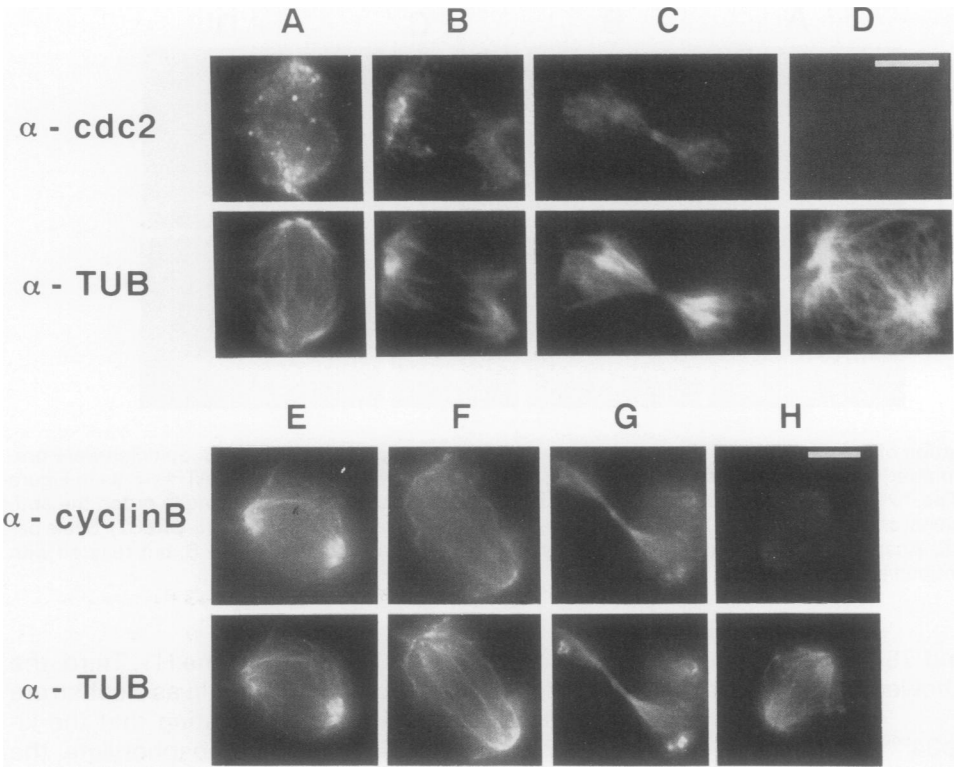

Figure 11. **Immunolocalization of p34^{cdc2}/cyclin B.** Spindles were processed for immunofluorescence using either polyclonal rabbit antibodies against the entire human p34^{cdc2} protein (α-cdc2) or human cyclin B (α-cyclin B) followed by a monoclonal antibody to β-tubulin (α-TUB). Scale bar is 10 μm. (A) Metaphase; (B) Anaphase; (C) Telophase; (D) Metaphase spindle processed for immunofluorescence without the primary anti-p34^{cdc2} antibody. (E) Metaphase; (F) Anaphase; (G) Telophase; (H) Metaphase spindle processed for immunofluorescence using preimmune cyclin B antiserum.

Although we have not completely purified the spindle kinase responsible for the phosphorylations seen here, we have no evidence that other kinases copurify or that any other major kinases routinely exist in or specifically associate with isolated spindles. We do not detect a Ca^{2+}/calmodulin-dependent protein kinase activity, as reported in sea urchin spindles (Dinsmore and Sloboda, 1988), although the spindle isolation procedure was different. The loss of kinase activity against histone H1, but the persistence of activity toward other substrates during mitosis, could be a result of a regulatory change to create a catalytically different form of one kinase rather than the existence of several kinases. Such a change in substrate specificity has been observed for p34^{cdc2} and is represented by a shift in native M_r, a complete loss of activity with histone H1, but continued activity toward other substrates such as casein (Brizuela *et al.,* 1989). A more detailed analysis of telophase and metaphase spindle kinase activities could address this issue.

Such an analysis may also further indicate the relationship of p34^{cdc2} to the partially purified spindle kinase. Our results suggest a similarity. The spindle kinase shows an abrupt loss of activity toward histone H1 and spindle substrates at anaphase onset, as reported for whole cell p34^{cdc2} (Draetta and Beach, 1988). The partially purified spindle kinase copurifies with a 34 000 M_r p34^{cdc2} immunoreactive species and a 56 000 M_r cyclin B immunoreactive species. However, the identification of many p34^{cdc2}-like kinases, such as eg1 and PHO85 (Toh-e *et al.,* 1988; Pines and Hunter, 1990; Paris *et al.,* 1991), necessitates caution in concluding that the spindle kinase is p34^{cdc2}.

Phosphorylation of some of the spindle kinase substrates reported here has been implicated but not demonstrated to regulate mitotic functions. It will be important to determine the sites of phosphorylation of MAP4, for example, the MT fiber protein, in relation to its proposed functional domains (Aizawa *et al.,* 1990, 1991; Chapin and Bulinski, 1991), and then to determine whether phosphorylation alters the assembly or stability dynamics of MTs, as has been reported for brain MAP phosphorylation (Jameson *et al.,* 1980). Phosphorylation of spindle-pole proteins, such as MAP1B (Vallee *et al.,* 1986), by the spindle kinase may promote MT nucleation, although MAP1B contains a MT-binding domain of a different class than MAP4 (Noble *et al.,* 1989; Hammarback *et al.,* 1991). There is evidence that phosphorylation is critical for such centrosomal function because the MPM-2 antibody can prevent the nucleation of

exogenous MTs in lysed cell models (Centonze and Borisy, 1990). Kinetochore spindle phosphoproteins have not been definitively identified, although the potential role for kinetochore phosphorylation in regulating MT capture and chromosome movement throughout mitosis is considerable. Recent analyses indicate that a protein kinase activity localized to the kinetochore of isolated chromosomes may activate (+)-end directed chromosome movement (Hyman and Mitchison, 1991). The continued investigation of mitotic motor molecules regulated by phosphorylation will be of great interest. Isolated spindles present a simplified model system containing all of the necessary components of mitotic centrosomes for assessing the role of specific protein phosphorylation on additional MT nucleation and assembly and perhaps on some aspects of chromosome function.

Materials and methods

Taxol was obtained from Dr. Matthew Suffness, NCI (Bethesda, MD). NP-40 detergent (SurfactAMPs) and bicinchoninic acid protein assay reagent were from Pierce (Rockford, IL). All other reagents were from Sigma (St. Louis, MO). Discontinuous SDS gel electrophoresis (Laemmli, 1970) and immunoblotting (Towbin *et al.*, 1979) were performed using the Mini Protean II system (Bio-Rad, Richmond, CA). We used 95% purity SDS (Sigma, L-5750) in particular to resolve α and β subunits of tubulin. Tris(hydroxymethyl)aminomethane (Tris)-buffered saline (TBS) consisted of 140 mM NaCl, 20 mM Tris, pH 7.4. Phosphate-buffered saline (PBSA) consisted of 137 mM NaCl, 3 mM KCl, 3 mM Na azide, and 10 mM Na K phosphate, pH 7.3.

Isolation and manipulation of spindles and cell extracts

CHO cells were cultured and synchronized in metaphase with a thymidine (5 mM)/nocodazole (0.13 μM) block as described (Kuriyama *et al.*, 1984), and spindles were isolated at varying times after release from nocodazole by lysing cells in a large excess of isolation medium, containing 2 mM Na piperazine-*N,N'*-bis(2-ethanesulfonic acid, pH 6.9, 0.5% NP-40, 10 μg/ml taxol, 0.1 mM EGTA, 0.1 mM dithiothreitol (DTT). Typically, metaphase spindles formed in cells 10 min after release from nocodazole, anaphase spindles at 20 min, and telophase at 30–40 min (see Figure 5A). Spindles were immediately concentrated out of lysis buffer by sedimentation in a clinical centrifuge for 20 min at 2000 $\times$ *g* and 4°C through 1 ml wash buffer onto a 50-μl cushion of 100% glycerol. Spindle wash buffer consisted of 30 mM *N*-2-hydroxyethylpiperazine-*N'*-2-ethanesulfonic acid (HEPES), pH 7.4, 20% glycerol, 20 mM β-glycerol phosphate, 0.5 mM DTT, 2 μg/ml taxol, 5 mM EGTA, 5 μg/ml CLAPS (1 μg/ml each: chymostatin, leupeptin, aprotinin, pepstatin, and soybean trypsin inhibitor). Spindles were resuspended in a minimal volume from the interface of the wash buffer and the glycerol cushion, and the resulting suspension was typically 50% glycerol and 0.5 mg/ml spindle protein. These spindles were stored at −20°C or −70°C and were stable in structure and kinase activity for ≥1 y.

Fractionation of the spindle protein kinase

All steps were performed at 4°C. Frozen spindles (see above) were concentrated by centrifugation in the TLS-55 swinging bucket rotor of a tabletop ultracentrifuge (Beckman, Palo Alto, CA) at 50 000 $\times$ *g* for 5 min onto a 100% glycerol cushion and resuspended to 20 mg/ml protein with column buffer (15 mM Hepes, 15 mM Tris, pH 7.4, 20% glycerol, 10 mM β-glycerol phosphate, 0.5 mM DTT, 1 mM EGTA, 1 μg/ml CLAPS). Spindles were extracted by dilution with an equal volume of column buffer containing 1.0 M NaCl, 10 μg/ml taxol on ice for 30 min. Spindles were immediately centrifuged (50 000 $\times$ *g*, 5 min) and the 0.5 M NaCl supernatant was diluted 10-fold with column buffer and directly adsorbed to DEAE-Sepharose CL-6B, which was washed with three-column volumes of column buffer and eluted with a linear gradient of NaCl from 0–1.0 M. Fractions were tested for OD_{280} and histone H1 kinase activity. Fractions of interest were pooled and concentrated with a Centricon-30 microconcentrator (Amicon, Danvers, MA), made 50% in glycerol, and stored at −70°C. Chromatography and processing resulted in losses of activity, but storage did not.

For gel filtration chromatography, the concentrated DEAE peak was loaded onto Sephacryl S-300 in <2% column volumn, eluted with column buffer + 0.1 M NaCl, and assayed for histone H1 kinase activity. Standards included β-amylase, alcohol dehydrogenase, albumin, carbonic anhydrase, and cytochrome c.

Protein kinase assay/autoradiography/ phosphoamino acid analysis

Protein kinase activity was assayed as previously described (Pelech *et al.*, 1988). Final volume was 25 μl, and standard conditions were 20 mM β-glycerophosphate, 0.1 mM NaOrthovanadate, 1 mM NaF, 30 mM K Hepes, pH 7.4, 10 mM MgAcetate, 1–50 μM ATP-γ-^{32}P at 2–6 dpm/pmole, 1 mM KEGTA, 1 mM DTT, 2 μg/ml CLAPS, 0.5 μM cAMP-dependent protein kinase inhibitor peptide. ATP-γ-^{32}P was purchased at ~3000 Ci/mmol, 3.3 μM (New England Nuclear-DuPont, Wilmington, DE). The reaction was performed at 30°C and terminated by pipetting 20 μl (80% of total volume) onto 2 $\times$ 2 cm squares of P81 phosphocellulose paper (Whatman, Clifton, NJ), and after 30 s, immersion into 1% phosphoric acid with five changes for 5 min each. P81 squares were counted in 4 ml Ecoscint (National Diagnostics, Manville, NJ). Kinase assays by SDS-polyacrylamide gel electrophoresis analysis were performed in the same manner, except that the reaction was stopped by dilution with an equal volume of 2$\times$ SDS sample buffer, immediately followed by boiling, as previously described (Tombes and Shapiro, 1987). Samples were either stored overnight at −20°C or run immediately, typically on 4–12% gradient polyacrylamide mini-gels (10 $\times$ 10 cm, 0.75-mm thickness). Silver staining was performed as described (Merril *et al.*, 1981). For autoradiography, dried gels were exposed to either X-Omat AR or Ortho M (Kodak, Rochester, NY) at either 25°C or −70°C between two intensifying screens (New England Nuclear-Dupont).

Phosphoamino acid analysis was performed as previously described (Lowndes *et al.*, 1990). Bands identified by autoradiography of one-dimensional SDS-polyacrylamide gels were excised and hydrolyzed with 6 N HCl for 1 h at 100°C. Supernatants from hydrolyzed gel slices were vacuum-dried, then resuspended with phosphoamino acid standards and electrophoresed on cellulose plates in 5% acetic acid/0.5% pyridine.

Protein kinase substrates

Calf thymus histone H1 was either from Boehringer Mannheim (Indianapolis, IN) or Type III-S from Sigma. Myelin basic protein and dephosphorylated casein were from Sigma. S6 peptide was modeled on the ribosomal protein S6 phosphate acceptor site (S6):RRLSSLRASTSKSEESQK and was provided by S. Pelech (Pelech *et al.,* 1988). Three-times cycled HeLa MTP was prepared as described (Bulinski and Borisy, 1980) and stabilized with 10 μg/ml taxol before HeLa MAPs were extracted with 0.5 M NaCl. Brain MAPs and tubulin were prepared by anion exchange chromatography from three-times cycled brain MTP as described (Murphy *et al.,* 1977). Further purification of brain MAPs was accomplished by sucrose density gradients. Five milliliters of 5–20% sucrose gradients were prepared in 50 mM NaPipes, 1 mM KEGTA, 0.5 mM DTT, 1 mM $MgCl_2$, 0.5 μg/ml CLAPS, overlaid with 0.5 ml MAPs, and centrifuged at 60 000 RPM for 12 h at 4°C in a SW65 ultracentrifuge rotor (Beckman). Any residual endogenous kinase activity in any of these fractions was eliminated either by diluting with an equal volume of 150 mM NaCl and boiling for 3 min or by alkylating with 5 mM NEM for 1 h at 45°C and quenching with 25 mM DTT at 20°C for 15 min.

Immunological methods

Anti-$p34^{cdc2}$ antibodies were a gift from Drs. Giulio Draetta and David Beach (Cold Spring Harbor Lab, NY). Drs. J. Pines and T. Hunter (The Salk Institute, San Diego, CA) provided antibodies against and standards for human cyclins A and B. Affinity purified anti-thiophosphoprotein monoclonal antibody was provided by Drs. M. Cyert and M. Kirschner through Dr. L. Wordeman (University of California, San Francisco) (Cyert *et al.,* 1988). Anti-centromere (CREST) antisera was provided by Drs. W.C. Earnshaw and R.L. Bernat (Johns Hopkins University, Baltimore, MD) (Bernat *et al.,* 1990). MAP1B monoclonal antibodies were obtained from Sigma (Riederer *et al.,* 1986). CHO MAP4 polyclonal antibodies were prepared and characterized as described (Vandre *et al.,* 1991). Dr. R. Kuriyama (University of Minnesota, Minneapolis, MN) provided the monoclonal antibody to CHO1 (Sellitto and Kuriyama, 1988).

Spindles were prepared for indirect immunofluorescence by centrifugation through 10 mM NaPipes, 1 mM KEGTA, 20% glycerol at 20°C for 15 min at 10 000 × *g* onto 0.1% poly L-lysine coated 12-mm circular glass coverslips (Bellco, Vineland, NJ). Coverslips were fixed in 100% methanol at −20°C for 3 min or 0.7% glutaraldehyde in PBSA for 5 min, in which case aldehyde autofluorescence was eliminated by 1 mg/ml $NaBH_4$ reduction for 10 min.

Antibody incubations were all for 30 min at 37°C in a volume of 40 μl contained between the coverslip and Parafilm. Antibodies were diluted with 0.1% bovine serum albumin (BSA)/TBS. Three washes of 5 min each in TBS alone were used between all steps. Blocking solution contained 10% normal goat serum in TBS (GIBCO, Grand Island, NY). Primary antibodies used were 1) monoclonal anti-β-tubulin, 1:500 (Amersham); 2) monoclonal anti-thiophosphoprotein, 1:500 (Cyert *et al.,* 1988); 3) polyclonal anti $p34^{cdc2}$ directed against C-terminus (Draetta and Beach, 1988) or entire recombinant human protein (Draetta *et al.,* 1987), both at 1:200; and 4) anti-human cyclin A or B, both at 1:200 dilutions (Pines and Hunter, 1990). Dual immunolabeling involved the sequential incubation of the first primary antibody, its secondary antibody, and its tertiary reagent before incubation with the second primary antibody and its secondary reagent. Secondary reagents included biotinylated affinity purified goat anti-human IgA + IgG + IgM (KPL, Gaithersburg, MD), biotinylated affinity purified goat anti-mouse IgG (KPL), biotinylated affinity purified goat anti-rabbit IgG (KPL), fluoresceinated affinity purified goat anti-rabbit IgG (KPL) and were typically used at 10 μg/ml. Texas Red conjugated streptavidin (KPL) was used at 5 μg/ml. Coverslips were mounted with Aqua Poly/Mount (Polysciences, Warrington, PA) and supplemented with 1 mg/ml p-phenylenediamine just before use.

Immunofluorescent images were obtained with a cooled CCD camera (Photometrics, Tucson, AZ) mounted on a Zeiss "Universal" microscope (Zeiss, Thornwood, NY). Images were acquired and processed under constant parameters using Image-1 software (Universal Imaging, Media, PA), then recorded onto T-MAX 100 film (Kodak).

Immunoblots were performed as described (Vandre *et al.,* 1991) using 10% methanol and no SDS for 1 h at 300 mA to transfer to 0.2 μm pore size nitrocellulose (Schleicher and Schuell, Keene, NH). Blocking and antibody incubation solutions contained 3% BSA, 0.05% Tween-20 in TBS. Secondary reagents included the biotinylated antibodies described above plus peroxidase conjugated streptavidin (KPL). 4-Cl naphthol 0.5 mg/ml and 0.05% H_2O_2 were used to develop blots. Primary antibodies were used at 1:500 ($p34^{cdc2}$, MPM-2, MAP4, MAP1B) and 1:1000 (cyclins) effective dilution from whole serum.

Quantitation of ^{32}P-incorporation and immunoreactivity was accomplished and calibrated as follows: dried gel bands containing proteins phosphorylated to different levels were excised, dissolved in scintillant, and counted to generate a standard curve. Optimal autoradiographic exposures and imaging conditions for densitometry of gels before excision of bands were determined by comparison with the standard curve generated from direct counting of phosphoproteins. Digital images were acquired for quantitative analysis by the use of an MTI Newvicon video camera (DAGE, Michigan City, IN) equipped with a Canon 50 mm Macro lens (Canon, Long Island, NY) over a homemade transilluminator and using Image-1 software (Universal Imaging). Although a standard curve was not determined for immunoblots, the optimal analogue and digital settings determined for autoradiograms were maintained and were used with reflected instead of transmitted light. Digital images were then recorded to T-MAX 100 film.

Acknowledgments

These experiments benefitted greatly from antibodies and standards provided by Drs. David Beach, Giulio Draetta, Martha Cyert, Marc Kirschner, Bill Earnshaw, Becky Bernat, Jonathon Pines, Tony Hunter, and Ryoko Kuriyama. We are extremely grateful to Dr. Victoria Centonze Frolich, who was instrumental in the preparation of CHO MAP4 antisera. Dr. Paul Bertics made available his expertise and equipment in phosphoamino acid analysis. The authors are grateful for advice from Drs. Victoria Centonze Frohlich, Laurent Meijer, Steve Pelech, and Dale Vandre. Drs. Gordon Hering and Gary Ward gave particularly insightful advice. Steve Limbach, Leanne Olds, and Mary Beth Tombes provided valuable and skillful illustrative assistance.

Received: May 15, 1991.
Revised and accepted: August 6, 1991.

References

Aizawa, H., Emori, Y., Mori, A., Murofushi, H., Sakai, H., and Suzuki, K. (1991). Functional analyses of the domain structure of microtubule-associated protein-4 (MAP-U). J. Biol. Chem. *266,* 9841–9846.

Aizawa, H., Emori, Y., Murofushi, H., Kawasaki, H., Sakai, H., and Suzuki, K. (1990). Molecular cloning of a ubiquitously distributed microtubule-associated protein with M_r 190,000. J. Biol. Chem. *265,* 13849–13855.

Ajiro, K., Shibata, K., and Nishikawa, Y. (1990). Subtype-specific cyclic AMP-dependent histone H1 phosphorylation at the differentiation of mouse neuroblastoma cells. J. Biol. Chem. *265,* 6494–6500.

Alfa, C.E., Ducommun, B., Beach, D., and Hyams, J.S. (1990). Distinct nuclear and spindle pole body populations of cyclin-cdc2 in fission yeast. Nature *347,* 680–692.

Bailly, E., Doree, M., Nurse, P., and Bornens, M. (1989). $p34^{cdc2}$ is located in both nucleus and cytoplasm; part is centrosomally associated at G2/M and enters vesicles at anaphase. EMBO J. *8,* 3985–3995.

Belenguer, P., Caizergues-Ferrer, M., Labbe, J.-C., Doree, M., and Amalric, F. (1990). Mitosis-specific phosphorylation of nucleolin by $p34^{cdc2}$ protein kinase. Mol. Cell. Biol. *10,* 3607–3618.

Belmont, L.D., Hyman, A.A., Sawin, K.E., and Mitchison, T.J. (1990). Real-time visualization of cell cycle-dependent changes in microtubule dynamics in cytoplasmic extracts. Cell *62,* 579–589.

Bernat, R.L., Borisy, G.G., Rothfield, N.F., and Earnshaw, W.C. (1990). Injection of anticentromere antibodies in interphase disrupts events required for chromosome movement at mitosis. J. Cell Biol. *111,* 1519–1533.

Bonifacino, J.S., Klausner, R.D., and Sandoval, I.V. (1985). A widely distributed nuclear protein immunologically related to the microtubule-associated protein MAP1 is associated with the mitotic spindle. Proc. Natl. Acad. Sci. USA *82,* 1146–1150.

Brizuela, L., Draetta, G., and Beach, D. (1989). Activation of human CDC2 protein as a histone H1 kinase is associated with complex formation with the p62 subunit. Proc. Natl. Acad. Sci. USA *86,* 4362–4366.

Bulinski, J.C., and Borisy, G.G. (1980). Microtubule-associated proteins from cultured HeLa cells: analysis of molecular properties and effects on microtubule polymerization. J. Biol. Chem. *255,* 11570–11576.

Centonze, V.E., and Borisy, G.G. (1990). Nucleation of microtubules from mitotic centrosomes is modulated by a phosphorylated epitope. J. Cell Sci. *95,* 405–411.

Chapin, S.J., and Bulinski, J.C. (1991). Non-neuronal 210 $\times 10^3$ M_r microtubule-associated protein (MAP4) contains a domain homologous to the microtubule-binding domains of neuronal MAP2 and tau. J. Cell Sci. *98,* 27–36.

Chou, Y.-H., Bischoff, J.R., Beach, D., and Goldman, R.D. (1990). Intermediate filament reorganization during mitosis is mediated by $p34^{cdc2}$ phosphorylation of vimentin. Cell *62,* 1063–1071.

Cyert, M.S., Scherson, T., and Kirschner, M.W. (1988). Monoclonal antibodies specific for thiophosphorylated proteins recognize *Xenopus* MPF. Dev. Biol. *129,* 209–216.

Davis, F.M., Wright, D.A., Penkala, J.E., and Rao, P.N. (1989). Mitosis-specific monoclonal antibodies block cleavage in amphibian embryos. Cell Struct. Funct. *14,* 271–277.

De Mey, J., Aerts, F., De Raeymaeker, M., Daneels, G., Moeremans, M., De Wever, B., Vandre, D.D., Vallee, R.B., Borisy, G.G., and De Brabander, M. (1987). Microtubule associated protein (MAP) 1A: a phosphoprotein associated with spindle fibers and microtubule organizing centres. In: Nature and Function of Cytoskeletal Proteins in Motility and Transport, Progress in Zoology, vol. 34, (ed. K.E. Wolhlfarth-Botterman), New York: Gustav Fischer Verlag, 187–205.

Dinsmore, J.H., and Sloboda, R.D. (1988). Calcium and calmodulin-dependent phosphorylation of a 62kd protein induces microtubule depolymerization in sea urchin mitotic apparatuses. Cell *53,* 769–780.

Draetta, G., and Beach, D. (1988). Activation of cdc2 protein kinase during mitosis in human cells: cell cycle-dependent phosphorylation and subunit arrangement. Cell *54,* 17–26.

Draetta, G., Brizuela, L., Potashkin, J., and Beach, D. (1987). Identification of p34 and p13, human homologs of the cell cycle regulators of fission yeast encoded by $cdc2^+$ and $suc1^+$. Cell *50,* 319–325.

Engle, D.B., Doonan, J.H., and Morris, N.R. (1988). Cell-cycle modulation of MPM-2 specific spindle pole body phosphorylation in *Aspergillus nidulans.* Cell Motil. Cytoskeleton *10,* 432–437.

Hammarback, J.A., Obar, R.A., Hughes, S.M., and Vallee, R.B. (1991). MAP1B is encoded as a polyprotein that is processed to form a complex N-terminal microtubule-binding domain. Neuron *7,* 1–20.

Heald, R., and McKeon, F. (1990). Mutations of phosphorylation sites in lamin A that prevent nuclear lamina disassembly in mitosis. Cell *61,* 579–589.

Hyman, A.A., and Mitchison, T.J. (1991). Two different microtubule-based motor activities with opposite polarities in kinetochores. Nature *351,* 206–211.

Jameson, L., Frey, T., Zeeberg, B., Dalldorf, F., and Caplow, M. (1980). Inhibition of microtubule assembly by phosphorylation of microtubule-associated proteins. Biochemistry *19,* 2472–2479.

Keryer, G., Davis, F.M., Rao, P.N., and Beisson, J. (1987). Protein phosphorylation and dynamics of cytoskeletal structures associated with basal bodies in *Paramecium.* Cell Motil. Cytoskeleton *8,* 44–54.

Kuang, J., Zhao, J.-Y., Wright, D.A., Saunders, G., and Rao, P.N. (1989). Mitosis-specific monoclonal antibody MPM-2 inhibits *Xenopus* oocyte maturation and depletes maturation-promoting activity. Proc. Natl. Acad. Sci. USA *86,* 4982–4986.

Kuriyama, R. (1989). 225-Kilodalton phosphoprotein associated with mitotic centrosomes in sea urchin eggs. Cell Motil. Cytoskeleton *12,* 90–103.

Kuriyama, R., Keryer, G., and Borisey, G.G. (1984). The mitotic spindle of Chinese hamster ovary cells isolated in taxol-containing medium. J. Cell Biol. *66,* 265–275.

Kuriyama, R., and Borisy, G.G. (1981). Microtubule-nucleating activity of centrosomes in Chinese hamster ovary cells is independent of the centriole cycle but coupled to the mitotic cycle. J. Cell Biol. *91,* 822–826.

Laemmli, U.K. (1970). Cleavage of structural proteins during the assembly of the head of bacteriophage T4. Nature *227,* 680–685.

Lamb, N.J.C., Fernandez, A., Watrin, A., Labbe, J.-C., and Cavadore, J.-C. (1990). Microinjection of $p34^{cdc2}$ kinase induces marked changes in cell shape, cytoskeletal organization, and chromatin structure in mammalian fibroblasts. Cell *60,* 151–165.

Langan, T., Gautier, J., Lohka, M., Hollingsworth, R., Moreno, S., Nurse, P., Maller, J., and Sclafani, R.A. (1989). Mammalian growth-associated H1 histone kinase: a homolog of $cdc2^+$/

CDC28 protein kinases controlling mitotic entry in yeast and frog cells. Mol. Cell. Biol. *9,* 3860–3868.

Lowndes, J.M., Hokin-Neaverson, M., and Bertics, P.J. (1990). Kinetics of phosphorylation of Na^+/K^+-ATPase by protein kinase C. Biochim. Biophys. Acta *1052,* 143–151.

Merril, C.R., Dunau, M.L., and Goldman, D. (1981). A rapid sensitive silver stain for polypeptides in polyacrylamide gels. Anal. Biochem. *110,* 201–207.

Moreno, S., and Nurse, P. (1990). Substrates for $p34^{cdc2}$: in vivo veritas? Cell *61,* 549–551.

Murphy, D.B., Vallee, R.B., and Borisy, G.G. (1977). Identity and polymerization-stimulatory activity of the nontubulin proteins associated with microtubules. Biochemistry *16,* 2598–2605.

Noble, M., Lewis, S., and Cowan, N.J. (1989). The microtubule binding domain of microtubule-associated protein MAP1B contains a repeated sequence motif unrelated to that of MAP2 and Tau. J. Cell Biol. *109,* 3367–3376.

Nigg, E.A., Schafer, G., Hilz, H., and Eppenberger, H.M. (1985). Cyclic-AMP-dependent protein kinase type II is associated with the golgi complex and with centrosomes. Cell *41,* 1039–1051.

Nurse, P. (1990). Universal control mechanism regulating onset of M-phase. Nature *344,* 503–508.

Paris, J., Le Guellec, R., Couturier, A., Le Guellec, K., Omilli, F., Camonis, J., MacNeill, S., and Phillipe, M. (1991). Cloning by differential screening of a *Xenopus* cDNA coding for a protein highly homologous to cdc2. Proc. Natl. Acad. Sci. USA *88,* 1039–1043.

Pelech, S.L., Tombes, R.M., Meijer, L., and Krebs, E.G. (1988). Activation of myelin basic protein kinases during echinoderm oocyte maturation and egg fertilization. Dev. Biol. *130,* 28–36.

Peter, M., Nakagawa, J., Doree, M., Labbe, J.C., and Nigg, E.A. (1990a). Identification of major nucleolar proteins as candidate mitotic substrates of cdc2 kinase. Cell *60,* 791–801.

Peter, M., Nakagawa, J., Doree, M., Labbe, J.C., and Nigg, E. (1990b). In vitro disassembly of the nuclear lamina and M phase-specific phosphorylation of lamins by cdc2 kinase. Cell *61,* 591–602.

Pines, J., and Hunter, T. (1990). Human cyclin A is adenovirus E1A-associated protein p60 and behaves differently from cyclin B. Nature (Lond) *346,* 760–763.

Rattner, J.B., Lew, J., and Wang, J.H. (1990). $p34^{cdc2}$ kinase is localized to distinct domains within the mitotic apparatus. Cell Motil. Cytoskeleton *17,* 227–235.

Riabowol, K., Draetta, G., Brizuela, L., Vandre, D., and Beach, D. (1989). The cdc2 kinase is a nuclear protein that is essential for mitosis in mammalian cells. Cell *57,* 393–401.

Riederer, B., Cohen, R., and Matus, A. (1986). MAP5: a novel brain microtubule-associated protein under strong developmental regulation. J. Neurocytol. *15,* 763–775.

Sellitto, C., and Kuriyama, R. (1988). Distribution of a matrix component of the midbody during the cell cycle in Chinese hamster ovary cells. J. Cell Biol. *106,* 431–439.

Shenoy, S., Choi, J.-K., Bagrodia, S., Copeland, T.D., Maller, J.L., and Shalloway, D. (1989). Purified maturation promoting factor phosphorylates $pp60^{c\text{-}src}$ at the sites phosphorylated during fibroblast mitosis. Cell *57,* 763–774.

Snyder, J.A., Hamilton, B.T., and Mullins, J.M. (1982). Loss of mitotic centrosomal microtubule initiation capacity at the metaphase-anaphase transition. Eur. J. Cell Biol. *27,* 191–199.

Theurkauf, W.E., and Vallee, R.B. (1982). Molecular characterization of the cAMP-dependent protein kinase bound to microtubule-associated protein 2. J. Biol. Chem. *257,* 3284–3290.

Toh-e, A., Tanaka, K., Uenoso, Y., and Wickner, R.B. (1988). PHO85, a negative regulator of the PHO system, is a homolog of the protein kinase gene, CDC28, of Saccharomyces cerevisiae. Mol. & Gen. Genet. *214,* 162–164.

Tombes, R.M., and Shapiro, B.M. (1987). Enzyme termini of a phosphorylcreatine shuttle: purification and characterization of two creatine kinase isozymes from sea urchin sperm. J. Biol. Chem. *262,* 16011–16019.

Towbin, H., Staehelin, T., and Gordon, J. (1979). Electrophoretic transfer of proteins from polyacrylamide gels to nitrocellulose sheets: procedure and some applications. Proc. Natl. Acad. Sci. USA *76,* 4350–4354.

Vallee, R.B., Bloom, G.S., and Luca, F.C. (1986). Differential structure and distribution of the high molecular weight brain microtubule-associated proteins, MAP-1 and MAP-2. Ann. NY Acad. Sci. *466,* 134–144.

Vandre, D.D., Davis, F., Rao, P., and Borisy, G. (1984). Phosphoproteins are components of mitotic microtubule organizing centers. Proc. Natl. Acad. Sci. USA *81,* 4439–4443.

Vandre, D.D., Davis, F.M., Rao, P.N., and Borisy, G.G. (1986). Distribution of cytoskeletal proteins sharing a conserved phosphorylated epitope. Eur. J. Cell Biol. *41,* 72–81.

Vandre, D.D., Centonze, V.E., Peloquin, J., Tombes, R.M., and Borisy, G.G. (1991). Proteins of the mammalian mitotic spindle: phosphorylation/dephosphorylation of MAP-4 during mitosis. J. Cell Sci. *98,* 577–588.

Verde, F., Labbe, J.-C., Doree, M., and Karsenti, E. (1990). Regulation of microtubule dynamics by cdc2 protein kinase in cell-free extracts of *Xenopus* eggs. Nature *343,* 233–238.

Ward, G., and Kirschner, M.W. (1990). Identification of cell cycle-regulated phosphorylation sites on nuclear lamin C. Cell *61,* 561–577.

Wordeman, L., Davis, F.M., Rao, P.N., and Cande, W.Z. (1989). Distribution of phosphorylated spindle-associated proteins in the diatom *Stephanopyxis turris.* Cell Motil. Cytoskeleton *12,* 33–41.

Zhao, J.-Y., Kuang, J., Adlakha, R.C., and Rao, P.N. (1989). Threonine phosphorylation is associated with mitosis in HeLa cells. FEBS Lett. *249,* 389–395.

Zieve, G., and Solomon, F. (1982). Proteins specifically associated with the microtubules of the mammalian mitotic spindle. Cell *28,* 233–242.